

Enhanced measurement precision with continuous interrogation during dynamical decoupling

Jun Zhang(张军), Peng Du(杜鹏), Lei Jing(敬雷), Peng Xu(徐鹏), Li You(尤力), and Wenxian Zhang(张文献)

Citation: Chin. Phys. B, 2024, 33 (**3**): 030301. DOI: 10.1088/1674-1056/ad1985
Journal homepage: http://cpb.iphy.ac.cn; http://iopscience.iop.org/cpb

What follows is a list of articles you may be interested in

Long-range interacting Stark many-body probes with super-Heisenberg precision

Rozhin Yousefjani, Xingjian He(何行健), and Abolfazl Bayat
Chin. Phys. B, 2023, 32 (**10**): 100313. DOI: 10.1088/1674-1056/acf302

Orientation determination of nitrogen-vacancy center in diamond using a static magnetic field

Yangpeng Wang(王杨鹏), Rujian Zhang(章如健), Yan Yang(杨燕), Qin Wu(吴琴), Zhifei Yu(于志飞), and Bing Chen(陈冰)
Chin. Phys. B, 2023, 32 (**7**): 070301. DOI: 10.1088/1674-1056/acc0f7

High-fidelity quantum sensing of magnon excitations with a single electron spin in quantum dots

Le-Tian Zhu(朱乐天), Tao Tu(涂涛), Ao-Lin Guo(郭奥林), and Chuan-Feng Li(李传锋)
Chin. Phys. B, 2022, 31 (**12**): 120302. DOI: 10.1088/1674-1056/ac8919

Fringe removal algorithms for atomic absorption images: A survey

Gaoyi Lei(雷高益), Chencheng Tang(唐陈成), and Yueyang Zhai(翟跃阳)
Chin. Phys. B, 2022, 31 (**5**): 050313. DOI: 10.1088/1674-1056/ac3758

Optical scheme to demonstrate state-independent quantum contextuality

Ya-Ping He(何亚平), Deng-Ke Qu(曲登科), Lei Xiao(肖磊), Kun-Kun Wang(王坤坤), and Xiang Zhan(詹翔)
Chin. Phys. B, 2022, 31 (**3**): 030305. DOI: 10.1088/1674-1056/ac229f

---

RAPID COMMUNICATION

Enhanced measurement precision with continuous interrogation during dynamical decoupling

Jun Zhang(张军)[1], Peng Du(杜鹏)[1], Lei Jing(敬雷)[1], Peng Xu(徐鹏)[1], Li You(尤力)[2], and Wenxian Zhang(张文献)[1,3,†]

[1] *Key Laboratory of Artificial Micro- and Nano-structures of Ministry of Education, and School of Physics and Technology, Wuhan University, Wuhan* 430072, *China*

[2] *State Key Laboratory of Low-Dimensional Quantum Physics, Department of Physics, Tsinghua University, Beijing* 100084, *China*

[3] *Wuhan Institute of Quantum Technology, Wuhan* 430206, *China*

(Received 5 October 2023; revised manuscript received 11 December 2023; accepted manuscript online 29 December 2023)

Dynamical decoupling (DD) is normally ineffective when applied to DC measurement. In its straightforward implementation, DD nulls out DC signal as well while suppressing noise. This work proposes a phase relay method that is capable of continuously interrogating the DC signal over many DD cycles. We illustrate its efficacy when applied to the measurement of a weak DC magnetic field with an atomic spinor Bose–Einstein condensate. Sensitivities approaching standard quantum limit or Heisenberg limit are potentially realizable for a coherent spin state or a squeezed spin state of 10000 atoms, respectively, while ambient laboratory level noise is suppressed by DD. Our work offers a practical approach to mitigate the limitations of DD to DC measurement and would find other applications for resorting coherence in quantum sensing and quantum information processing research.

Keywords: quantum sensing, continuous interrogation, quantum magnetometer, dynamical decoupling, Heisenberg limit

PACS: 03.65.Yz, 03.67.Bg, 67.85.–d **DOI:** 10.1088/1674-1056/ad1985

1. Introduction

As one of the most studied control methods, dynamical decoupling (DD) can actively suppress noise to preserve coherence of a quantum system,[1,2] e.g., in trapped ions,[3–7] solid-state spins,[8–15] superconducting quantum circuits,[16–18] and ultracold atomic gases.[19–22] Despite its successes, DD has found only a few usages in precision measurement of a DC signal.[23] While unwanted and unknown stochastic noises are suppressed by periodically refocusing a quantum state to the initial one with DD,[19,24] a DC (or low frequency AC) signal sensed from phase interrogation by a quantum state provides no net accumulated phase.[25] Such a dilemmatic situation is unfortunate, especially since the effect of achieving beyond standard quantum limit (SQL) precision could obviously benefit from entangled or squeezed quantum states that are otherwise easily decohered.[26–32]

This work studies the application of DD to precision measurement by suppressing noise while reaping up a gain from continuous sensing of a weak DC (or low frequency AC) signal.[25] To explain our idea, let us recall an athlete in a 5–10–5 shuttle run. After start, his/her displacement increases while running forward. When he/she comes around after touching the turn-around lines, however, the displacement with respect to the initial line decreases and eventually becomes zero upon returning back to the start line, although the net distance covered continuously grows after repeated line touchings at both ends. Analogously, the interrogated signal and the accompanying noise accumulate during the first half of a DD cycle, but are both compensated for by the complementary second half period. To obtain a net phase accumulation of a DC signal, one could simply flip the signal's phase but not that of the noise during the second half as illustrated in Fig. 1, provided the signal was known. Such a simple (alternately repeated) phase flip could help to recover the DC signal by allowing the consequent interrogation to last for many DD cycles while the noise remains suppressed. We refer the above described manipulation protocol as the phase relay method (PRM). If implemented this way, DD, which has been demonstrated successfully for high frequency AC signal measurements in a variety of physical systems,[4,14,15,19,24,33–38] will also be applicable to the measurement of DC (and low-frequency AC) signals.

2. Continuous interrogation during DD

We illustrate the PRM by applying it to measure a weak DC magnetic field using an atomic spinor Bose–Einstein condensate through Ramsey interferometry.[39] The condensate is assumed to consist of $N = 10000$ ^{87}Rb atoms, which comes with a strong repulsive spin independent interaction in addition to a weak ferromagnetic spin exchange interaction. For small or moderate sized N and with the condensate in an optical trap, its Hamiltonian under the single spatial mode approx-

†Corresponding author. E-mail: wxzhang@whu.edu.cn

© 2024 Chinese Physical Society and IOP Publishing Ltd

imation reduces to $H = -c_2' \boldsymbol{J}^2 + \gamma \boldsymbol{B} \cdot \boldsymbol{J}$, after constant terms are dropped,[40,41] where c_2' denotes the spin exchange interaction strength with the collective condensate spin $\boldsymbol{J} = \sum_{i=1}^{N} \boldsymbol{F}_i$ from spin $\boldsymbol{F}_i$ for ith atom, γ the atomic gyromagnetic ratio, and $\boldsymbol{B}$ the total magnetic field which possibly includes a fixed known bias field $\boldsymbol{B}_0$, a fixed weak but unknown DC magnetic field $\boldsymbol{b}_0$ (the signal to be measured), and stray stochastic magnetic field $\boldsymbol{b}$ (noise) to be suppressed by DD. We consider the simple case of the bias and the signal field along the same z-axis direction, while the stray field is randomly directed with random amplitude ($|\boldsymbol{b}| < b_c$ upto a cutoff amplitude b_c).

2.1. Noise suppression with uniaxial DD

The condensate spin decoheres by the stray magnetic field, which eventually limits the optimal achievable sensitivity of the magnetometer. Although the dephasing noise model may give analytical results as derived in Appendix B, we consider a more realistic stray-field model. Including the stray magnetic field, the Hamiltonian becomes

$$H = -c_2' \boldsymbol{J}^2 + \gamma(B_0 + b_0) J_z + \gamma(b_x J_x + b_y J_y + b_z J_z), \quad (1)$$

where $b_{x,y,z} \in [-b_c, b_c]$ and a bias field $B_0 \gg b_{0,c}$ is required. To suppress decoherence from the stray field, many DD schemes can be applied.[2,42–50] We adopt a uniaxial DD protocol which is robust and easy to implement experimentally.[51]

Here we emphasize that the spin exchange term $c_2' J^2$ is the natural ingredient of the spinor BEC, and thus it can not be excluded from the Hamiltonian (1), even though it has no contribution to the results of our calculation. Specifically, we consider a ferromagnetic interaction $c_2' < 0$, which ensures the validity of the single mode approximation utilized in deriving the system Hamiltonian.

By denoting the π-pulse along x-axis by X, the evolution operator for a unit cycle becomes $U_{2\tau} = X U_\tau X U_\tau = \exp(-\mathrm{i}2\tau\bar{H})$, where $U_\tau = \exp(-\mathrm{i}\tau H)$ with τ the duration between pulses and $\bar{H}$ the time averaged Hamiltonian over a whole cycle. Under the magic condition $\tau = 2m\pi/(\gamma B_0)$ (for $m = 1, 2, 3, \ldots$), the uniaxial DD is capable of efficiently suppressing decoherence from the stray magnetic field, because the effective coupling between the condensate spin and the stray magnetic field is reduced by a factor of (b_z/B_0), leading to $\bar{H} \approx -c_2' \boldsymbol{J}^2 + (b_z/B_0)\gamma b_y J_y$.[51] Further suppression of the stray magnetic field is achieved if a refined uniaxial DD protocol, the balanced uniaxial DD (BUni-DD) $[X\bar{U}_\tau X \bar{U}_\tau X U_\tau X U_\tau]$, is employed, where U_τ ($\bar{U}_\tau$) denotes free evolution with a positive (negative) bias field. The latter leads to the BUni-DD period $T = 4\tau$ and the magic condition $\gamma B_0 \tau = 2m\pi$ remains needed. It is easy to find that the average Hamiltonian further improves to $\bar{H} \approx -c_2' \boldsymbol{J}^2 + O((b_c/B_0)^2)$.

2.2. Phase relay method

To estimate the signal field amplitude with Ramsey interferometry, the condensate spin is initially prepared to align along x-direction. During the interrogation time t, it processes along the direction of the bias and signal field sum which provides an accumulated time phase $\phi = \gamma(B_0 + b_0)t$ with $B_0 = |\boldsymbol{B}_0|$ and $b_0 = |\boldsymbol{b}_0|$. By measuring precisely this phase ϕ at time t, the signal field can be determined. Experimentally, this is accomplished by measuring J_y, the y-component of the collective spin, which oscillates with time as shown in Fig. 1. The estimated phase between 0 and 2π is extracted by fitting the observed data to a sinusoidal function. For longer interrogation time, this phase will exceed 2π. Consequently, one would hope to keep track of indexing the number of oscillation cycles in order to continuously interrogate a monotonically increased phase instead of a zigzagged one chopped into $[0, 2\pi]$. During interrogation, the stray magnetic field stochastically disturbs the measured phase and introduces an uncertainty $\Delta\phi$, which leads to an uncertainty in the signal Δb_0. Such effects from the stray magnetic field can be suppressed by periodically executed DD pulses, for example, with instantaneous π rotations of the spin along x-axis, or spin flips. As numerical results verified in Fig. 1, effects of the noise are indeed suppressed significantly. Unfortunately, the interrogated phase from the bias plus the signal field is also refocused by the above DD pulses, i.e., the net phase accumulation after complete cycles of DD diminishes, making it difficult to estimate the signal field.

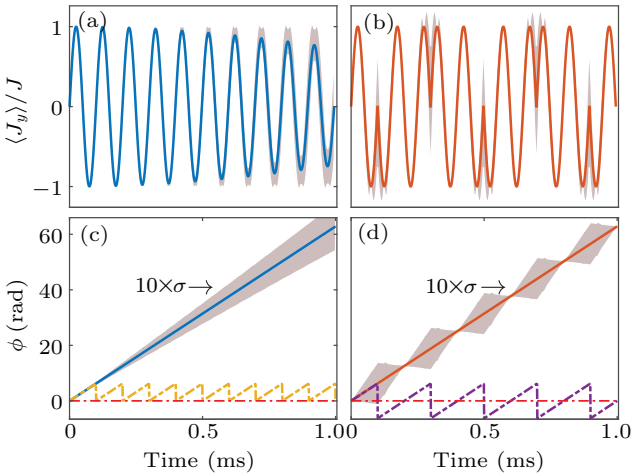


Fig. 1. Phase relay method. (a) Numerically simulated mean (blue solid line) and the standard deviation (gray shaded region) for observable J_y without DD. (b) The same as in (a) but with DD shown by the red solid line (mean) and the gray shaded region (one standard deviation). The applied pulse interval is $\tau = 0.1$ ms. The standard deviation is found to be strongly suppressed after one DD cycle $T = 4\tau$. (c) Phase ϕ extracted directly from the simulation (a) (yellow dash-dotted line) and with hypothetical accumulation taking into account the indexed number of oscillations (blue solid line). The standard deviation of the phase (shaded in gray) is multiplied by 10 for better viewing. The phase increases linearly and the standard deviation grows monotonically with time. (d) Phase extracted directly from the experimental observable (b) (purple dash-dotted line) and after applying the PRM (red solid line). The standard deviation of the phase (shaded gray) is multiplied by 100. Similarly, the phase after PRM increases linearly and the standard deviation is strongly suppressed after each DD cycle.

While BUni-DD protocol discussed above suppresses the stray magnetic field, the signal field is also suppressed unfortu-

nately as the accumulated phase nearly zeros out after each DD cycle. However, the signal field differs from the stray magnetic field because it is by definition nonzero and we further note that the pulse interval for the DD pulse sequence τ is exactly known. These features (knowledge) provide us an opportunity to continuously accumulate the phase associated with the signal by the phase relay method (PRM), inspired by the 5–10–5 shuttle run.

We now examine the interrogated phase accumulation associated with the signal in the first DD cycle, over a period of 4τ (see Fig. 2). For the sake of clarity, we neglect the stray magnetic field at this stage. During the first quarter, the phase of the signal $\phi_s(\tau) = \gamma b_0 \tau$ accumulates linearly. At $t = \tau$, an instantaneous X pulse then flips the condensate spin and the phase changes to $-\phi_s(\tau)$. During the second quarter, the signal's phase evolves linearly back to 0, i.e., $\phi_s(2\tau) = 0$. This phase pattern repeats in the third and the fourth quarters as in the first and the second quarters, respectively. The total interrogated phase during a whole DD cycle vanishes.

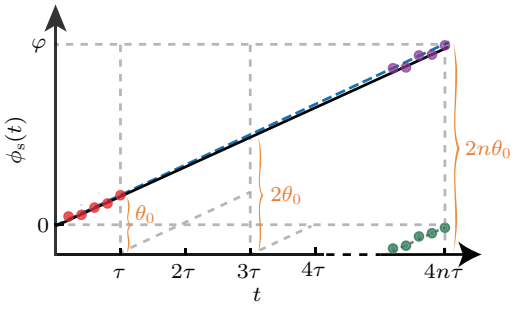


Fig. 2. The PRM protocol. A roughly estimated phase-shift θ_0 is obtained by linear least square fitting (red dots) to a few data points extracted from preliminary measurements of the observable during the first quarter period. One then extracts estimated phases $\phi_s(t)$ (green dots) and shifts them according to θ_0 and the cycle indexing number n (purple dots), during the whole BUni-DD sequence. The blue dashed line illustrates the relayed phase based on the preliminary estimated θ_0. An improved estimate for θ_0 is obtained by a least square linear fit to all the relayed data from many BUni-DD cycles (black line). The slope of the fitted black line denotes a refined estimate of the signal field b_0.

As shown in Fig. 2, an immediate method to continuously interrogate the signal phase during the BUni-DD cycle is to shift the phase during $t \in [\tau, 3\tau]$ by a fixed amount θ_0 and by $2\theta_0$ during the last quarter $t \in [3\tau, 4\tau]$ respectively, provided $\theta_0 = \gamma b_0 \tau$ from the signal field b_0 was known. For the nth DD cycle, the required phase shift of the first quarter becomes $(2n-2)\theta_0$, the second and the third quarter $(2n-1)\theta_0$, and the fourth quarter $2n\theta_0$. In practice, we would first obtain a crude estimate to the phase shift θ_0 by running a few preliminary experiments without DD pulses, then followed by optimizations, and finally determine θ_0 more precisely. One plausible approach is shown in Fig. 2 which obtains the shifted phase data (by varying θ_0) during the first and the last quarters of the whole DD sequence, and optimizes with least square fitting. Afterwards, a refined and more accurate θ_0 may be determined and likewise the signal field is determined more precisely.

Including the stray magnetic field, our numerical simulations confirm that the PRM remains effective. For practical implementations, the PRM protocol can be summarized explicitly by the following steps.

(i) Take a few measurements of $\langle J_y \rangle$ to obtain $\langle J_y \rangle(t)$ at short time.

(ii) Extract the phase $\phi_s(t)$ from the experiment data, fit linearly the phase–time curve, and find out a crude estimate for the phase-shift θ_0, which is similar to the adjustment of fire in military.

(iii) Take more measurements of $\langle J_y \rangle(t)$ at the beginning, in the middle, and at the end of the BUni-DD sequence.

(iv) Extract phases $\phi_s(t)$ from the larger data set, and relay/shift measured phases accordingly with the knowledge of the cycle indexing number n and θ_0.

(v) Optimize θ_0 with a least-square linear fit.

(vi) Derive the signal field b_0.

With the PRM, the phase relays continuously during a DD cycle, as shown schematically in Fig. 1, which can be further optimized by least square fitting the data over many DD cycles. Consequently, the net phase from the bias and signal fields continuously integrates while the stochastic contributions from noise are averaged out after repeated DD cycles, thus the measurement precision of a weak DC signal is enhanced.

3. Heisenberg limit magnetometer with spin squeezing

To evaluate the achievable precision after an interrogation time t, we calculate the signal-field sensitivity for measuring the weak magnetic field according to

$$\eta = \frac{\Delta J_y}{|\partial J_y/\partial \phi|\gamma\sqrt{t}},$$

which usually diverges at very short time as stochastic uncertainty from the stray field is yet to become effective.[33,37,38] In order to achieve quantum enhanced sensitivity, it is necessary to consider metrologically useful entangled states such as the spin squeezed states (SSS).[29] In the absence of stray field, an SSS is capable of approaching the Heisenberg limit (HL) scaling, i.e., $\eta_{\rm HL} < \eta < 2\eta_{\rm HL}$, where $\eta_{\rm HL} = 1/(\gamma J\sqrt{t})$ (see Appendix A for detail derivation).[26,27]

We consider an SSS with averaged spin point along the x-axis, while the squeezing direction is along the y-axis, orthogonal to the averaged spin. Such a state is readily prepared experimentally in a spinor ^{87}Rb atomic condensate.[28,52,53] We set $\omega_0 = \gamma B_0 = 2\pi \times 10$ kHz corresponding to a bias field of $B_0 = 14.3$ mG ($\gamma = 0.70$ MHz/G). The cutoff field is taken to be at a nominal laboratory noise level $b_c = 0.1$ mG (with an angular frequency $2\pi \times 70$ Hz). As for the signal, we assume $b_0 = 1.6$ μG, which serves to demonstrate quantum enhanced

precision. The pulse interval of BUni-DD is $\tau = 0.1$ ms, satisfying the magic condition $\omega_0\tau = 2\pi$. After repeated simulation runs with random stray magnetic field $\boldsymbol{b}$ of uniformly distributed components $b_{x,y,z} \in [-b_c, b_c]$, we compute the observable $\langle J_y \rangle$ and its standard deviation, extract the phase, derive the signal's phase and its standard deviation, and finally determine the sensitivity η (Fig. 3).

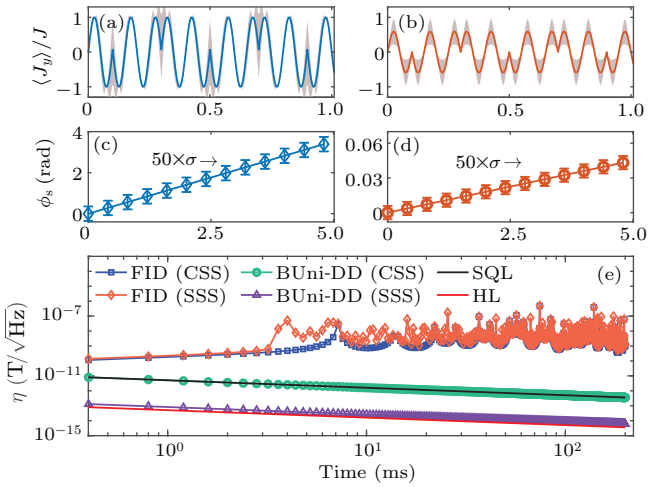


Fig. 3. Precision measurement of a weak DC magnetic field with DD. (a), (b) The average condensate spins (solid lines) and their standard deviations (gray shaded areas) for initial coherent spin state (CSS) versus squeezed spin state (SSS). (c), (d) The signal's phases ϕ_s extracted with PRM from simulated experimental observables in (a) and (b), respectively with $b_0 = 160$ μG in (c) and $b_0 = 1.6$ μG in (d). The bias and the cutoff fields are assumed to be $B_0 = 14.3$ mG and $b_c = 0.1$ mG, respectively. The small standard deviations are multiplied by 50 in order to be clearly visible. (e) The signal field's sensitivities under DD for CSS (green circles) and SSS (purple triangles), respectively approaching the SQL (black solid line) and HL (red solid line). For comparison, we present the sensitivities without DD pulses for both CSS (blue squares) and SSS (red diamonds) as well in the same figure. The DD pulses are seen to strongly suppress noise and significantly improve sensitivity.

Although an entangled SSS can enhance sensing sensitivity, in practice this is difficult because an entangled state is fragile to stray magnetic field. Figure 4(a) shows the sensitivity under free evolution within 1 ms, which decoheres quickly such that no quantum enhancement is observed. The oscillations of sensitivity arise due to the periodicity in Eq. (A7) and the optimal value is found to be limited by ~ 100 pT/$\sqrt{\text{Hz}}$. Therefore, it is crucial to efficiently suppress the stray magnetic field for sensing a weak signal field, especially when entangled probe states are used.

By applying BUni-DD pulses and performing the PRM to the SSS, we obtain much higher sensitivity going beyond SQL and approaching HL within 200 ms, at about 6 fT/$\sqrt{\text{Hz}}$ for 10000 atoms. The projected sensitivity continuously improves with prolonged interrogation time. As shown in Fig. 4(b), the sensitivity for the SSS reaches its optimum ~ 4 fT/$\sqrt{\text{Hz}}$ at $t \sim 770$ ms. The simulation results show clear quantum enhancement.

To investigate the dependence of sensitivity on the noise field strength, we change the cutoff field b_c from 10^{-9} mG to 1 mG, but fix the interrogation time at $t = 200$ ms while keeping other parameters the same as those in Fig. 3. The optimal sensitivity at low noise level is found to settle at about 6 fT/$\sqrt{\text{Hz}}$ and is independent of b_c (Fig. 5). The sensitivity deteriorates rapidly with increasing noise strength once b_c is larger than a threshold, which is found to be approximately $1/(\gamma t J) \sim 10^{-7}$ mG without DD pulses but becomes $(B_0/b_c)^2/(\gamma t\sqrt{J}) \sim 0.1$ mG with DD pulses. Although the SSS is fragile to the stray field, the DD implemented with our PRM supports its application to precision measurement at common laboratory noise level ($b_c \sim 0.1$ mG).[19,54]

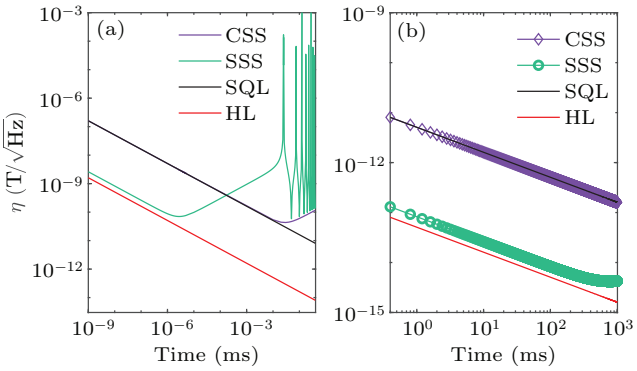


Fig. 4. Sensitivity at short and long times for CSS (purple line) and SSS (green line). The cutoff field assumed $b_c = 0.1$ mG. Both states decohere quickly without the application of BUni-DD (a) but maintain their coherence for longer times with the application of BUni-DD (b). The black and the red lines denote SQL and HL, respectively.

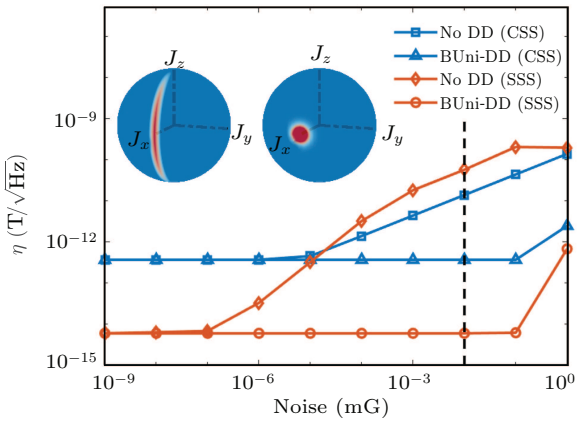


Fig. 5. Optimal sensitivities within 200 ms of interrogation time at different noise levels. The optimal sensitivities detected by an initial CSS with (without) DD pulses are denoted by blue triangles (squares); the ones detected by an initial SSS with (without) DD pulses are shown with orange circles (diamonds). As long as the stray magnetic field is lower than the noise threshold ~ 0.1 mG, noise is strongly suppressed and sensitivities with DD are independent of the noise strength. For comparison, the noise thresholds without DD pulses are numerically found to be $\sim 10^{-6}$ mG for an initial CSS and $\sim 10^{-8}$ mG for an initial SSS. The vertical line marks a laboratory noise level of 0.01 mG.[19]

As for an initial quantum state without entanglement between atoms, such as coherent spin state (CSS), the optimal sensitivity follows the SQL in the absence of stray magnetic field. Similarly, the CSS decoheres within 0.1 ms in the presence of stray field, as shown in Fig. 4(a). However, after the application of BUni-DD with PRM, the sensitivity of CSS is found to reach SQL in the same noisy environment.

Assuming the same number of atoms and averaged spin direction as the SSS, we achieve the sensitivity 0.36 pT/$\sqrt{\text{Hz}}$ for sensing a signal field $b_0 = 160$ μG. This result compares favorably to a previously reported experimental result of 0.5 pT/$\sqrt{\text{Hz}}$ with $N \sim 10^6$ atoms for a unity duty cycle.[55] As shown in Fig. 4(b), the sensitivity for CSS keeps tracking SQL within an interrogation time of 1 s, due to the application of BUni-DD and PRM. In addition, the threshold of noise strength that impairs the sensitivity of a CSS is approximately $1/(\gamma t\sqrt{J}) \sim 10^{-5}$ mG without DD pulses, but lifts up to $(B_0/b_c)^2/(\gamma t\sqrt{J}) \sim 0.1$ mG with DD pulses.

4. Discussion and conclusion

In conclusion, we propose the PRM which enables continuous interrogation during DD and enhances the system's coherence during quantum measurements. With this PRM, we numerically show that the sensitivity of a spinor-BEC-based magnetometer approaches the SQL with an initial CSS and the HL with an SSS. Remarkably, the simulated optimal sensitivity with only 10000 atoms enters the regime of a few fT/$\sqrt{\text{Hz}}$ within 200 ms interrogation time, indicating the great potential of enhanced quantum metrology utilizing the spin squeezing and the metrologically-useful-quantum entanglement. The PRM applies not only to the investigated spinor-BEC magnetometer,[19,20] but also to other quantum sensor systems suffering severe decoherence, such as nitrogen vacancy centers in diamond,[8–10,12,13,15] trapped ions,[4–6] and superconducting quantum devices.[16,17]

Three concerns are experimentally related. (i) At a first glance, the relative stability of the bias field b_0/B_0 is roughly 0.01%. Although such a highly stable magnetic field has been realized in recent experiments, where the bias magnetic field is of the order of ~ 1 G and stabilized to a range from 10 μG to 0.1 mG,[7,52,53] we note that the magnetic field stability is actually characterized by the stray magnetic field. Thus the ratio b_c/B_0 is about 1%, which is quite easy to realize. (ii) The rapid reversion of the bias field (in the order of ~ 1 μs) was achieved in experiments without introducing adiabatic Landau–Zener transitions between atoms in different spin components.[56] Therefore we may neglect the short reversion time of the bias field during our numerical simulations. (iii) To measure $\langle J_y\rangle$ in a spin-1 BEC experiment, one may employ continuous measurement using magneto-optical imaging techniques,[55] or projective measurement using the Stern–Gerlach technique after an additional $\pi/2$ pulse which rotates the condensate spin to z direction.[52]

For the purpose of a concise illustration of PRM, we have assumed several idealizations for the magnetic field sensitivities to reach the HL. Specifically, the sensitivity calculations do not take into account any dead time during state-preparation and measurement stage, and assume hard pulses with instantaneous and perfect rotation. Therefore, the sensitivities achieved in practical experiments are not as prominent as predicted here. Nevertheless, our results point out the possibility to suppress noises with DD for a DC magnetometer using PRM. It is worthwhile to design more robust pulse sequences accounting for pulse width and shape, in order to meet practical requirements.

Appendix A: Parameter estimation and sensitivity

Under the single mode approximation,[40] the Hamiltonian for the magnetometer based on atomic spin-1 Bose–Einstein condensate is given by

$$H = -c_2' \boldsymbol{J}^2 + \gamma \boldsymbol{B}\cdot\boldsymbol{J}, \tag{A1}$$

where c_2' represents the spin exchange interaction strength, $\boldsymbol{J} = \sum_{i=1}^{N} \boldsymbol{s}_i$ the collective atomic spin of the condensate, and $\boldsymbol{s}_i$ the spin operator for the ith atom, $\gamma = (2\pi)0.70$ MHz/G the gyromagnetic ratio, and $\boldsymbol{B}$ the total magnetic field which includes a DC magnetic field b_0 (signal), stray magnetic field b (noise), and possibly a bias B_0. The direction and magnitude of the DC field are fixed, while they are random for the stray field.

With the (to be estimated) signal magnetic field b_0 assumed static and pointed along the z-axis, the Hamiltonian in the absence of stray field reduces to $H_0 = -c_2' \boldsymbol{J}^2 + \gamma b_0 J_z$. To estimate b_0, a polarized initial state $\psi(0)$, e.g., a coherent spin state (CSS) with its average spin along x-direction taking the maximum collective spin value $\langle J_x\rangle = J$ is prepared. It evolves under H_0 for an interrogation time t and becomes $\psi(t) = \exp(-\mathrm{i}[-c_2' t\boldsymbol{J}^2 + \phi_s J_z])\psi(0)$, where $\phi_s = \gamma b_0 t$ is the accumulated dynamical phase from the signal field b_0. One can determine b_0 by measuring a dependent observable, for instance, $\langle J_y\rangle$, which gives $\langle J_y\rangle(t) = J\sin(\phi_s)$. According to parameter estimation theory, the value of b_0 can be estimated from the measured $\langle J_y\rangle(t)$ through the relation

$$b_0 = \frac{1}{\gamma t}\arcsin\left(\frac{\langle J_y\rangle(t)}{J}\right). \tag{A2}$$

The variance of the measurement data limits the uncertainty of b_0. The minimal detectable magnetic field for an interrogation time t is thus found to be

$$\Delta b_0 = \frac{1}{\gamma t}\frac{\Delta J_y}{|\partial\langle J_y\rangle(t)/\partial\phi_s|}, \tag{A3}$$

where $\Delta J_y = \sqrt{\langle J_y^2\rangle - \langle J_y\rangle^2}$ denotes the standard deviation. When M uncorrelated consecutive measurements are carried out for a total measurement time $T = Mt$, the minimal detectable field becomes

$$\Delta b_0 = \frac{1}{\gamma}\frac{1}{\sqrt{tT}}\frac{\Delta J_y}{|\partial\langle J_y\rangle(t)/\partial\phi_s|}. \tag{A4}$$

The sensitivity for such a magnetometer is defined as

$$\eta = \Delta b_0 \sqrt{T} = \frac{1}{\gamma}\frac{1}{\sqrt{t}}\frac{\Delta J_y}{|\partial\langle J_y\rangle/\partial\phi_s|}. \tag{A5}$$

This indicates that a longer coherence time corresponds to achieving better sensitivity. It is straightforward to find that the optimal sensitivity for an initial CSS is given by

$$\eta_C(t) = \frac{1}{\gamma}\frac{1}{\sqrt{2tJ}}, \tag{A6}$$

which reaches the standard quantum limit (SQL) with respect to the spin size J following the scaling $1/\sqrt{J}$.

The sensitivity for a squeezed spin state (SSS) with average spin pointed along the same x-direction exhibiting optimal squeezing along y-direction is given by

$$\eta_S(t) = \frac{1}{\gamma}\frac{\theta(t)}{\lambda}\frac{\sqrt{\xi_s^2}}{\sqrt{2tJ}}, \tag{A7}$$

where $\theta(t) = \sqrt{1+\tan^2(\omega t)(\langle\Delta^2 J_x\rangle_0/\langle\Delta^2 J_y\rangle_0)}$ corresponds to the fixed direction measurement (e.g., y-direction) and $\langle\cdots\rangle_0$ denotes the average over the initial state. It is important to point out that the optimal squeezing direction remains perpendicular to the averaged spin for such an SSS during the Larmor precession in a magnetic field along z-axis. Nevertheless, the optimal squeezing direction is difficult to track experimentally, so we measure spin squeezing in the fixed y-direction. $\lambda = |\langle J_x\rangle_0|/J$ represents the ratio of the average initial spin to the total spin size, with $\lambda = 1$ for a CSS and $\lambda \approx 0.58$ for the SSS at $J = 10000$ respectively. Following Kitagawa and Ueda,[57] we define spin squeezing parameter $\xi_s^2 = 2\min(\Delta^2 J_y)/J$, which gives $\xi_s^2 = 1$ for a CSS and $\xi_s^2 \approx 0.91/J$ for the SSS at $J = 10000$ in a spin-1 atomic Bose–Einstein condensate (as considered in the main text). At $\theta(t) = 1$, we find

$$\eta_S \approx \frac{1.6}{\gamma}\frac{1}{\sqrt{2t}\,J},$$

an optimal sensitivity that scales as $1/J$, which is beyond SQL and approaches to the Heisenberg limit (HL). The scaling with respect to J manifests the quantum enhancement to measurement precision by using SSS.

Appendix B: Free evolution in dephasing noises

To facilitate analytical derivation, we consider the dephasing model in which the stray field distributes uniformly within $[-b_c, b_c]$ only along z-direction. The system Hamiltonian becomes $H = -c_2' \boldsymbol{J}^2 + \gamma b_z J_z + \gamma b_0 J_z$, where b_z denotes the z-component of the stray magnetic field.

It is easy to calculate straightforwardly the evolution of $\langle J_y\rangle$ for an initial CSS with spin initially polarized along x-direction, which follows

$$\langle J_y\rangle(t) = J\sin(\omega_s t)\frac{\sin(\omega_c t)}{\omega_c t}, \tag{B1}$$

with $\omega_{s/c} = \gamma b_{0/c}$. The cutoff Larmor frequency ω_c characterizes a dephasing time $T_2^* \sim \omega_c^{-1}$. The variance $(\Delta J_y)^2$ can be divided into a quantum and a classical part

$$(\Delta J_y)^2(t) = (\Delta J_y)_Q^2(t) + (\Delta J_y)_C^2(t), \tag{B2}$$

where

$$(\Delta J_y)_Q^2(t) = \frac{J}{4}\left[1+\cos(2\omega_s t)\frac{\sin(2\omega_c t)}{2\omega_c t}\right], \tag{B3}$$

$$(\Delta J_y)_C^2(t) = \frac{J^2}{2}\left[1-\cos(2\omega_s t)\frac{\sin(2\omega_c t)}{2\omega_c t} - 2\sin^2(\omega_s t)\frac{\sin^2(\omega_c t)}{(\omega_c t)^2}\right]. \tag{B4}$$

At ultrashort time when $\omega_c t \ll 1$, only the quantum part plays a role because $(\Delta J_y)_Q^2(t) \approx (J/4)[1+\cos(2\omega_s t)]$ while $(\Delta J_y)_C^2(t) \approx 0$. As time goes by, the classical part becomes more and more important and eventually dominates at long time for large J. Similar to the results shown in Fig. 1(a), $\langle J_y\rangle(t)$ exhibits decayed oscillations, while the standard deviation ΔJ_y increases with time, according to Eqs. (B1) and (B2).

Acknowledgements

Project supported by the NSAF (Grant No. U1930201), the National Natural Science Foundation of China (Grant Nos. 12274331, 91836101, and 91836302), the National Key R&D Program of China (Grant No. 2018YFA0306504), and Innovation Program for Quantum Science and Technology (Grant No. 2021ZD0302100). The numerical calculations in this paper have been partially done on the supercomputing system in the Supercomputing Center of Wuhan University.

References

[1] Viola L, Knill E and Lloyd S 1999 *Phys. Rev. Lett.* **82** 2417
[2] Suter D and Álvarez G A 2016 *Rev. Mod. Phys.* **88** 041001
[3] Biercuk M J, Uys H, VanDevender A P, Shiga N, Itano W M and Bollinger J J 2009 *Phys. Rev. A* **79** 062324
[4] Kotler S, Akerman N, Glickman Y, Keselman A and Ozeri R 2011 *Nature* **473** 61
[5] Bohnet J G, Sawyer B C, Britton J W, Wall M L, Rey A M, Foss-Feig M and Bollinger J J 2016 *Science* **352** 1297
[6] Kaewuam R, Tan T R, Arnold K J, Chanu S R, Zhang Z and Barrett M D 2020 *Phys. Rev. Lett.* **124** 083202
[7] Wang P, Luan C Y, Qiao M, Um M, Zhang J, Wang Y, Yuan X, Gu M, Zhang J and Kim K 2021 *Nat. Commun.* **12** 233
[8] Petta J, Johnson A, Taylor J, Laird E, Yacoby A, Lukin M, Marcus C, Hanson M and Gossard A 2005 *Science* **309** 2180
[9] Liu R B, Yao W and Sham L J 2007 *New J. Phys.* **9** 226
[10] Cappellaro P, Jiang L, Hodges J S and Lukin M D 2009 *Phys. Rev. Lett.* **102** 210502
[11] de Lange G, Wang Z H, Ristè D, Dobrovitski V V and Hanson R 2010 *Science* **330** 60
[12] Medford J, Cywiński L, Barthel C, Marcus C M, Hanson M P and Gossard A C 2012 *Phys. Rev. Lett.* **108** 086802
[13] Rong X, Geng J, Wang Z, Zhang Q, Ju C, Shi F, Duan C K and Du J 2014 *Phys. Rev. Lett.* **112** 050503

[14] Schmitt S, Gefen T, Stürner F M, Unden T, Wolff G, Müller C, Scheuer J, Naydenov B, Markham M, Pezzagna S, Meijer J, Schwarz I, Plenio M, Retzker A, McGuinness L P and Jelezko F 2017 *Science* **356** 832

[15] Zopes J, Sasaki K, Cujia K S, Boss J M, Chang K, Segawa T F, Itoh K M and Degen C L 2017 *Phys. Rev. Lett.* **119** 260501

[16] Nakamura Y, Pashkin Y A, Yamamoto T and Tsai J S 2002 *Phys. Rev. Lett.* **88** 047901

[17] Bylander J, Gustavsson S, Yan F, Yoshihara F, Harrabi K, Fitch G, Cory D G, Nakamura Y, Tsai J S and Oliver W D 2011 *Nat. Phys.* **7** 565

[18] Pokharel B, Anand N, Fortman B and Lidar D A 2018 *Phys. Rev. Lett.* **121** 220502

[19] Eto Y, Ikeda H, Suzuki H, Hasegawa S, Tomiyama Y, Sekine S, Sadgrove M and Hirano T 2013 *Phys. Rev. A* **88** 031602

[20] Muessel W, Strobel H, Linnemann D, Hume D B and Oberthaler M K 2014 *Phys. Rev. Lett.* **113** 103004

[21] Trypogeorgos D, Valdés-Curiel A, Lundblad N and Spielman I B 2018 *Phys. Rev. A* **97** 013407

[22] Anderson R P, Kewming M J and Turner L D 2018 *Phys. Rev. A* **97** 013408

[23] In contrast to coupling all the spin levels during a pulse, remarkably, Kaewuam *et al.* demonstrated an exquisite strategy for dynamical decoupling implemented in multi-ion clock system, where a pulse only couples upper hyperfine levels of a clock transition to cancel out inhomogeneous broadening associated with the electric quadrupole shift induced by neighboring ions.[6]

[24] Hirose M, Aiello C D and Cappellaro P 2012 *Phys. Rev. A* **86** 062320

[25] We note that the low frequency AC signal fields are specified as those with a characteristic time much longer than the measurement time.

[26] Giovannetti V, Lloyd S and Maccone L 2004 *Science* **306** 1330

[27] Esteve J, Gross C, Weller A, Giovanazzi S and Oberthaler M K 2008 *Nature* **455** 1216

[28] Hamley C D, Gerving C S, Hoang T M, Bookjans E M and Chapman M S 2012 *Nat. Phys.* **8** 305

[29] Pezzè L, Smerzi A, Oberthaler M K, Schmied R and Treutlein P 2018 *Rev. Mod. Phys.* **90** 035005

[30] Kaubruegger R, Silvi P, Kokail C, van Bijnen R, Rey A M, Ye J, Kaufman A M and Zoller P 2019 *Phys. Rev. Lett.* **123** 260505

[31] Bao H, Duan J, Jin S, Lu X, Li P, Qu W, Wang M, Novikova I, Mikhailov E E, Zhao K F, Molmer K, Shen H and Xiao Y 2020 *Nature* **581** 159

[32] Baamara Y, Sinatra A and Gessner M 2021 *Phys. Rev. Lett.* **127** 160501

[33] Taylor J M, Cappellaro P, Childress L, Jiang L, Budker D, Hemmer P R, Yacoby A, Walsworth R and Lukin M D 2008 *Nat. Phys.* **4** 810

[34] Aiello C D, Hirose M and Cappellaro P 2013 *Nat. Commun.* **4** 1419

[35] Wolf T, Neumann P, Nakamura K, Sumiya H, Ohshima T, Isoya J and Wrachtrup J 2015 *Phys. Rev. X* **5** 041001

[36] Lang J E, Liu R B and Monteiro T S 2015 *Phys. Rev. X* **5** 041016

[37] Boss J M, Cujia K S, Zopes J and Degen C L 2017 *Science* **356** 837

[38] Degen C L, Reinhard F and Cappellaro P 2017 *Rev. Mod. Phys.* **89** 035002

[39] DC signal here refers to a static (or low frequency) magnetic field to be measured, while an observable such as spin average is oscillating with a (high) Larmor frequency.

[40] Law C K, Pu H and Bigelow N P 1998 *Phys. Rev. Lett.* **81** 5257

[41] The quadratic Zeeman shift for ^{87}Rb scales as 72 Hz/G^2, resulting negligible quadratic energy for our calculation at a typical magnetic field ($\sim$ 10 mG).

[42] Hahn E L 1950 *Phys. Rev.* **80** 580

[43] Meiboom S and Gill D 1958 *Rev. Sci. Inst.* **29** 688

[44] Solomon I 1959 *Phys. Rev. Lett.* **2** 301

[45] Viola L, Knill E and Lloyd S 1999 *Phys. Rev. Lett.* **82** 2417

[46] Uhrig G S 2007 *Phys. Rev. Lett.* **98** 100504

[47] Cywiński L, Lutchyn R M, Nave C P and Das Sarma S 2008 *Phys. Rev. B* **77** 174509

[48] Uhrig G S 2009 *Phys. Rev. Lett.* **102** 120502

[49] Haeberlen U 1976 *High Resolution NMR in Solids Selective Averaging* (New York: Academic Press)

[50] Zhang J, Han Y, Xu P and Zhang W 2016 *Phys. Rev. A* **94** 053608

[51] Yao Q, Zhang J, Yi X F, You L and Zhang W 2019 *Phys. Rev. Lett.* **122** 010408

[52] Luo X Y, Zou Y Q, Wu L N, Liu Q, Han M F, Tey M K and You L 2017 *Science* **355** 620

[53] Zou Y Q, Wu L N, Liu Q, Luo X Y, Guo S F, Cao J H, Tey M K and You L 2018 *Proc. Natl. Acad. Sci. USA* **115** 6381

[54] Gross C, Zibold T, Nicklas E, Esteve J and Oberthaler M K 2010 *Nature* **464** 1165

[55] Vengalattore M, Higbie J M, Leslie S R, Guzman J, Sadler L E and Stamper-Kurn D M 2007 *Phys. Rev. Lett.* **98** 200801

[56] Kell A, Link M, Breyer M, Hoffmann A, Köhl M and Gao K 2021 *Rev. Sci. Instr.* **92** 093202

[57] Kitagawa M and Ueda M 1993 *Phys. Rev. A* **47** 5138